Preparation, Characterization, and Release Behavior of Nanocomposite Microparticles Based on Polystyrene and Different Layered Silicates

Paola Scarfato,[1,2] Pietro Russo,[3] Domenico Acierno[3]

[1]*Department of Industrial Engineering, University of Salerno, 84084 Fisciano (Salerno), Italy*
[2]*Research Centre NANO_MATES (Nanomaterials and Nanotechnology), University of Salerno, 84084 Fisciano (Salerno), Italy*
[3]*Department of Materials and Production Engineering, University of Naples "Federico II," 80125 Napoli, Italy*

Received 28 April 2011; accepted 28 April 2011
DOI 10.1002/app.34783
Published online 11 August 2011 in Wiley Online Library (wileyonlinelibrary.com).

ABSTRACT: A microparticulated, organic–inorganic hybrid system, useful as an active agent carrier, was successfully developed with an emulsification/solvent evaporation method. The system consisted of nanostructured polystyrene microparticles containing different silicates as nanosized fillers and benzophenone (BP) as a model active substance. The adopted preparation procedure gave high yields of microparticles, which displayed regular geometry and high encapsulation efficiency of the active agent. X-ray diffraction measurements showed that all of the hybrid systems had a polymer–silicate intercalated morphology and the BP was molecularly dispersed in the microspheres. Moreover, preliminary *in vitro* release tests evidenced that the inclusion of the nanodispersed silicates into the polymer matrix significantly modified the release behavior of BP, depending on the silicate type. Therefore, the nanocomposite microparticles are of great potential in the field of controlled release. © 2011 Wiley Periodicals, Inc. J Appl Polym Sci 122: 3694–3700, 2011

Key words: microencapsulation; nanocomposites; polystyrene

INTRODUCTION

Microencapsulation is a widely used strategy for delivering active molecules in numerous industrial sectors, such as pharmaceuticals, cosmetics, agrochemicals, and textiles.[1–6] The key to success of the microencapsulation is in its huge versatility, which arises from the multitude of manufacturing techniques and materials available for the process. Thanks to that, microencapsulated formulations can meet multifaceted demands, for example, extension of the active agent effects, reduction of toxicity, protection against degradation in specific environments, control and targeting of release, masking of odor and/or taste of the active agent, and increase of the bioavailability of poor soluble active agents. However, the overall performance of a microencapsulated system and, then, its controlled release (CR) are strictly related to the chemicophysical character of the active substance, its affinity with the others materials used in the formulation, and the method of manufacture.[2,7–9]

In the search for CR systems, more and more flexible and tunable inorganic–organic hybrids have lately attracted interest because they can allow the safe retention and controlled delivery of various active agents into targets with high efficiency.[10–13] In particular, in recent years, many efforts have been directed toward the fabrication of polymer nanocomposite hybrids for the CR of drugs or other active agents.[14–18] In fact, it is well-known that the intimate mixing of polymers with inorganic clays or silica on a nanometer scale can lead to composite materials with bulk properties synergistically derived from raw components.[19] Despite the high prospects offered by polymer–silicate nanocomposite systems for CR applications, until today, very few data have been reported in the literature on the preparation and release behavior of microencapsulated devices based on these matrices.[20–22]

In this work, we performed a study (1) to investigate the possibility of realizing nanocomposite microparticles containing different natural or organomodified lamellar silicates in a polymer matrix and (2) to verify whether the inclusion of these nanometric silicates could be useful in modulating the release behavior of the hybrid formulations.

For this purpose, in this work, we prepared, by the sonication/solvent evaporation of an oil-in-water emulsion, polystyrene (PS)–silicate nanocomposites microparticles containing benzophenone (BP) as a model active agent and different types and amounts of silicates. In particular, the silicates used were a natural montmorillonite (MMT), an organomodified

Correspondence to: P. Scarfato (pscarfato@unisa.it).

MMT, and a natural mica (M). All of these clay minerals have a large specific surface area and good absorbability, cation-exchange capacity, and drug-carrying capability, and therefore, they are common ingredients as excipients in pharmaceutical products.[23]

The obtained PS–silicate nanocomposite microparticles were preliminarily analyzed to gain information about the encapsulation efficiency, morphology, and particle size distribution (PSD). Afterward, they were characterized by means of several techniques [small-angle X-ray diffraction (SAXD), thermogravimetric analysis (TGA), UV–visible spectroscopy, etc.] to obtain information about their nanostructure and release behavior.

EXPERIMENTAL

Materials

PS was purchased by Scientific Polymers Products (SP^2, Inc., Ontario, Wayne, NY). Poly(vinyl alcohol) (80% hydrolyzed), BP [$C_{13}H_{10}O$, melting temperature (T_m) = 48.5°C], and chloroform ($CHCl_3$) were analytical-reagent grade and were purchased from Sigma Aldrich S.r.l. (Milano, Italy). Natural sodium MMT ($d_{001} = 11.7$ Å) and organomodified sodium MMT Cloisite 10A (10A; $d_{001} = 19.2$ Å) were supplied by Southern Clay Products Inc. (Gonzales, TX), and M ($d_{001} = 9.8$ Å) was supplied by 20 Microns Ltd. (Vadodara, India).

Preparation of the microspheres

PS–silicate nanocomposite microparticles, with or without drug embedded, were prepared according to a standard procedure involving ultrasonication followed by the solvent evaporation of an oil-in-water emulsion. Typical preparation was performed by the dissolution of 2.0 g of polymer in 20 mL of $CHCl_3$ and the dispersion into the obtained solution of different amounts of silicate (MMT, 10A, or M at 3, 6, and 9 wt %) and drug (20 wt % of the matrix weight, if necessary). The suspension was stirred magnetically and sonicated in a water bath for 20 min to promote polymer intercalation between the silicate layers. Then, this oily phase was emulsified in 150 mL of water containing 0.2 g of poly (vinyl alcohol) with a T25 UTRA-TURRAX emulsifier (IKA, Staufen, Germany) at 2000 rpm for 2 min. Agitation was maintained until the $CHCl_3$ evaporated, and so this created solid particles suspended in the water. The suspension was filtered through a standard sieve and washed with water to yield a free-flowing powder. Following the same procedure, neat PS microparticles were also prepared for comparison. The neat PS and the PS–silicate nanocomposite microparticles were with the polymer or silicate abbreviation followed by x/y, where x denotes the silicate weight content and y denotes the drug weight content in the samples.

Drug content, microencapsulation yields, and encapsulation efficiency

Samples (5 mg) of three batches of microspheres were dissolved in 5 mL of $CHCl_3$, sonicated for 5 min, and centrifuged for 10 min at 300 rpm. The BP concentration was determined in the surnatant solutions with UV measurements. The UV spectra of BP were recorded on a PerkinElmer Lambda 800 spectrometer (PerkinElmer Italia, Monza, Italy) in the range 200–800 nm. Each analysis was made in triplicate, and the results expressed are average values.

The production yield is expressed as the weight percentage of the final product compared to the total amount of polymer and drug used in the microencapsulation experiment.

The encapsulation yield was calculated from the ratio of the actual amount to the theoretical amount of drug in the dry microparticles, where the theoretical drug content (%) was defined as the ratio between the mass of drug used in the preparation procedure (0.4 g) and the total mass of the microcapsule sample (2.4 g) and the actual drug content (%) was defined as the ratio between the mass of drug measured in the microcapsule sample by UV spectrometry and the total mass of the microcapsule sample (2.4 g).

Thermal analysis

TGA was performed with a TA Instruments Q500 apparatus (Vimodrone, Italy), with the microparticle specimens heated up to 900°C in an N_2 atmosphere at 20°C/min.

Size distribution of the microspheres

Microcapsules were analyzed for their size distribution. Dried particles were dispersed in distilled water containing 1 wt % Tween 20 surfactant and sonicated in a water bath for 1 min before sampling. Particle size analysis was obtained with a Beckman Coulter LS13 320 laser diffraction particle size analyzer (Milano, Italy), which detected particles in the range 0.4–2000 μm. The mean values and the standard deviations of the PSD curves are reported in Table I.

Microscopy

Scanning electron microscopy (SEM) micrographs were obtained with an EVO MA 10 apparatus (Carl Zeiss Italia S.p.A., Arese, Italy). The samples, sprinkled onto double-sided carbon adhesive tape that had previously been secured on aluminum stubs, were coated with an AuPd alloy with a high-vacuum sputter coater before analysis.

TABLE I
Actual Silicate and Drug Contents, Encapsulation Yields, and PSDs for the Hybrid Microparticles

Sample	Actual silicate content (%)[a]	Actual drug content (%)[b]	Encapsulation yield (%)	PSD (μm)[c]
PS 0/0	0	0	—	17 ± 11
MMT 3/0	2.9	0	—	23 ± 15
MMT 6/0	5.9	0	—	25 ± 17
MMT 9/0	8.7	0	—	18 ± 12
M 3/0	2.8	0	—	16 ± 11
M 6/0	5.7	0	—	12 ± 8
M 9/0	8.6	0	—	12 ± 9
10A 6/0	6.1	0	—	18 ± 10
PS 0/20	0	15.3	92	13 ± 10
MMT 6/20	5.8	14.0	84	15 ± 9
M 6/20	5.7	16.8	100	11 ± 8
10A 6/20	6.0	16.9	100	16 ± 9

[a] From TGA measurements.
[b] From UV spectrometry.
[c] From laser diffraction measurements.

X-ray diffraction (XRD)

SAXD spectra were recorded with a Rigaku D-MAX X-ray diffractometer (Tokyo, Japan) with Ni-filtered Cu Kα radiation (40 kV, 200 mA).

In vitro drug release

Release profiles of BP were determined with sink conditions provided in a SOTAX AT Smart Apparatus (Basel, Switzerland) online with a UV spectrophotometer (Spectracomp 602, Advanced Products srl, Milan, Italy) and a USP 28 dissolution test apparatus (n.2 paddle, 100 rpm). The measurements were performed in phosphate-buffered saline solution containing 1 wt % Tween 80 at 25°C for 4 h. All of the dissolution–release tests were done in triplicate; only the mean values are reported in the graph (standard deviations $< 5\%$). Samples of microspheres containing about 5 mg of BP were analyzed spectrophotometrically at $\lambda = 262$ nm.

RESULTS AND DISCUSSION

PS–silicate microparticles, with and without the drug, were preliminarily characterized to evaluate the actual silicate content in the hybrids, the actual drug content, and the microencapsulation yield. The average values are reported for each sample in Table I. The data show that the differences between the nominal and the measured silicate levels in the hybrids were less than 7%; this indicated that the preparation procedure used to obtain the microspheres guaranteed a satisfactory control of the sample composition. Moreover, for all of the systems, the actual drug content was very near to the theoretical one, and high microencapsulation yields were always obtained.

The morphology of the samples was examined by SEM. Figure 1 shows the SEM images of PS0/0, MMT 6/0, MMT 6/20, M 6/0, 10A 6/0, and 10A 6/20 microspheres, chosen as an example. All of the samples consisted of isolated microparticles with a spherical shape and nonporous surface. Most of the systems were quite smooth, except those containing natural sodium MMT in the formulation, which had a higher roughness and lower morphological uniformity. Moreover, the PSDs of the nanocomposite systems appeared to be bimodal; in fact, the SEM pictures evidenced the presence of a wider population of microparticles with small diameters (<1 μm), which might have resulted from a process involving the breakup of large particles during the solvent evaporation from the emulsion.

To verify that the silicates were dispersed on a nanometric scale in the PS matrix, SAXD analyses were carried out on the hybrid systems, with and without the drug. The diffractograms, reported in Figure 2, showed a shift of the basal spacing of the neat silicates toward lower 2θ values. This suggested that polymer chains were intercalated between the silicate layers in our experimental conditions; this gave an increase of the interstratic gap for all of the samples. However, in the case of the 10A-based systems, the diffractometric original basal peak of the silicate did not disappear; this indicated that this silicate was only partially intercalated, even when its expanded interlayer distance was higher compared to those of the other silicates.

The confinement of the PS chains between the silicate platelets markedly improved the thermal resistance of the nanocomposites, even at the lowest silicate percentages. Figure 3(a,b) compares the maximum decomposition temperatures (DT_{max}'s) of the microparticles with different compositions. The histogram of Figure 3(a) shows that the DT_{max} values of the nanocomposite microparticles increased about 10–

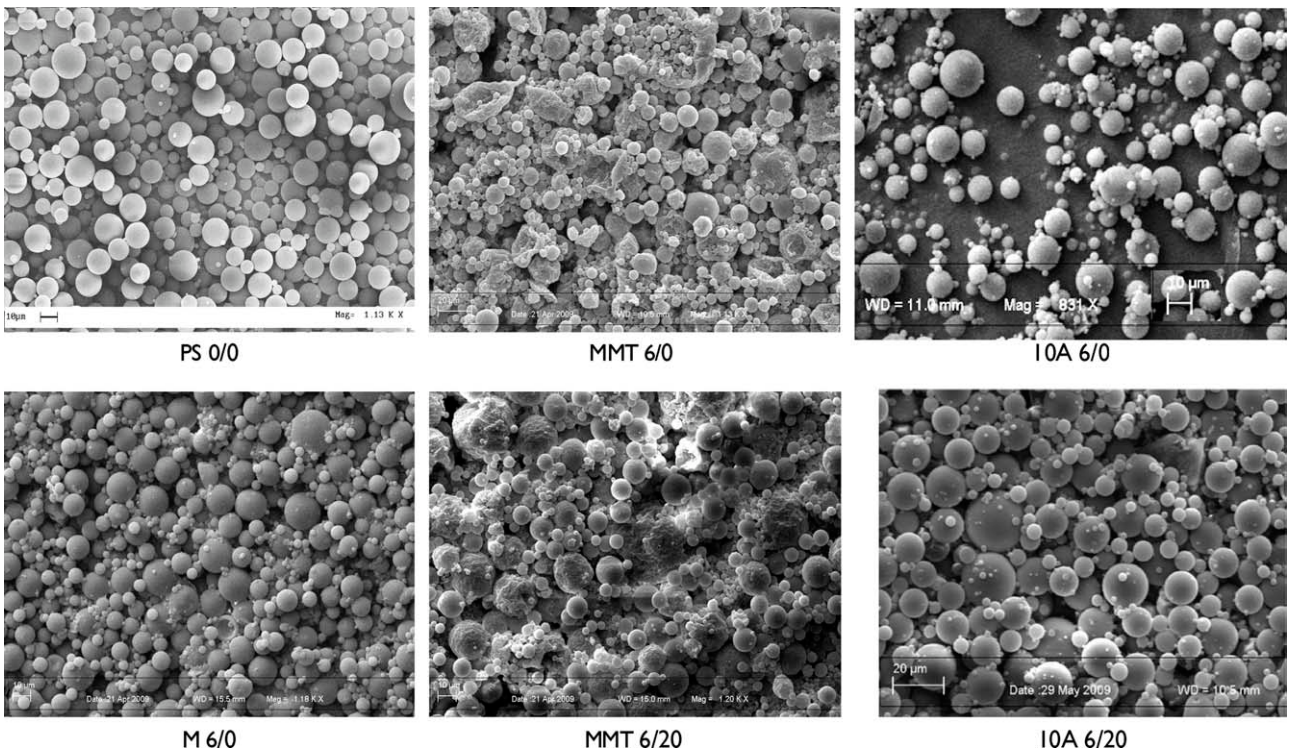

Figure 1 SEM images of some PS–silicate nanocomposite microspheres at different compositions.

25°C, depending on the silicate nature and percentage. The highest DT_{max} values were obtained for MMT- and 10A-based systems, which also showed the longest interlayer distances. Moreover, Figure 3(b) shows that the BP presence in the formulation contributed to further improve the thermal resistance of the nanocomposite microparticles, thanks to the thermostabilizer ability of BP. In particular, the DT_{max} values increased more than 10°C in the cases of the M- and MMT-based formulations, whereas no significant changes were measured for the 10A-based systems. The causes of the different thermostabilizer ability of BP in the analyzed formulations still need to be clarified, although it is reasonable to assume that they may be related to the different distribution levels at the nanoscale of the silicates and to the different chemical affinity among the polymer, silicate, and drug. On the other hand, the DT_{max} value of the PS 0/20 microcapsules was essentially unaffected by the BP presence. In this regard, it was reasonable to hypothesize that BP, having a low T_m ($T_m = 48.5$°C) and a high volatility, was completely evaporated from the PS 0/20 system at the degradation temperature, so no stabilizing effect was detectable.

With the aim of investigating whether the BP was molecularly dispersed in the microspheres, like a solid solution, XRD tests were performed. Figure 4 compares the XRD profiles of all of the BP-loaded microparticles of the neat PS and PS nanocomposite at 6 wt % silicate with that of crystalline neat BP. The diffractograms revealed that BP incorporation into the PS matrix, in our experimental conditions, reduced the crystallinity of BP to practical insignificance. Two factors could have contributed to this result: (1) the obtainment of a solid BP/PS solution because of their high chemical affinity and (2) the penetration and entrapment of the BP molecules between the silicate layers.

These two factors could have affected the release behavior of the microparticles in a complex way. On one hand, the obtainment of a solid solution could have effectively enhanced the solubility of crystalline and poorly soluble molecules such as BP, as has been proven for other release systems;[24] on the other hand, the development of chemical interactions between the BP and the PS matrix or the silicate platelets could have slowed down the release kinetics of the penetrant molecule from the microparticles toward the external medium.

To evaluate the overall effect of both the system formulation and the internal morphology on the release characteristics of the nanocomposite microparticles, preliminary *in vitro* release tests were carried out in phosphate-buffered saline solution at 25°C, according the USP procedure. The dissolution profiles are plotted in Figure 5, together with that of neat BP, which is reported for comparison. The graph shows that the confinement of the BP into the PS matrix delayed its release and that the incorporation of the nanosilicates into the formulations further contributed to slow down the release process, to an extent that depended on the silicate nature, and changed progressively in the following order: M < MMT < 10A. In particular, the effect

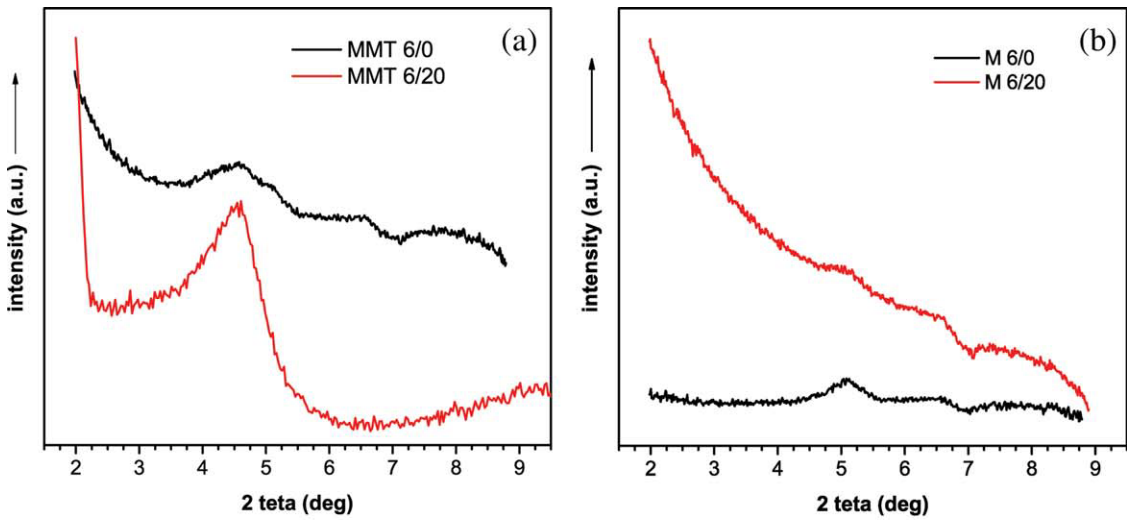

Interlayer spacing values (angstrom)		
MMT	MMT 6/0	MMT 6/20
11.7	19.1	19.2

Interlayer spacing values (angstrom)		
Mica	Mica 6/0	Mica 6/20
9.8	17.2	17.9

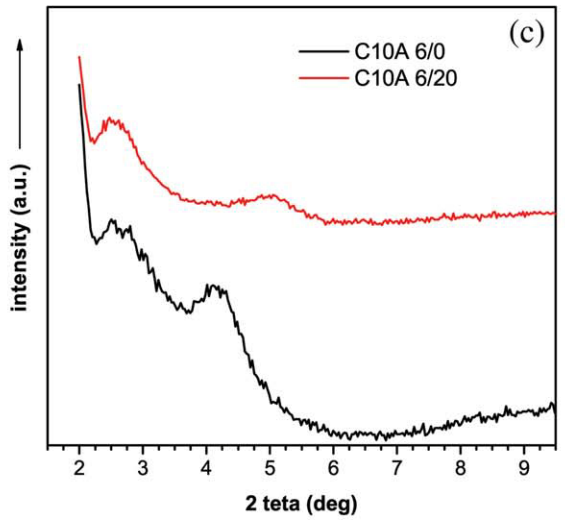

Interlayer spacing values (angstrom)		
C10A	C10A 6/0	C10A 6/20
--	34.8	35.3
19.2	21.1	17.7

Figure 2 SAXD diffractograms and corresponding silicate interlayer spacing values of the PS–silicate nanocomposite microspheres at different compositions. [Color figure can be viewed in the online issue, which is available at wileyonlinelibrary.com.]

increased with both (1) the intercalation degree of the polymer into the silicate [i.e., it was higher for systems with higher silicate interlayer spacing; see Fig. 2(a–c)] because increasing the intercalation degree also increased the diffusional path tortuosity of the penetrant molecules across the matrix and (2) the silicate–BP chemical affinity, which was higher in the case of the 10A organomodified clay.

To investigate the mode of release from the microcapsules, the release data were analyzed with the Higuchi equation:[25]

$$Q = k_H t^{1/2}$$

where Q is the percentage of BP released at time t and k_H is the Higuchi rate constant. The Higuchi plots reported in Figure 6 were found to be of good linearity with high correlation coefficients; these indicated that the drug-release mechanism from all of these microcapsules was essentially diffusion controlled, as could be expected because the PS matrix was insoluble.

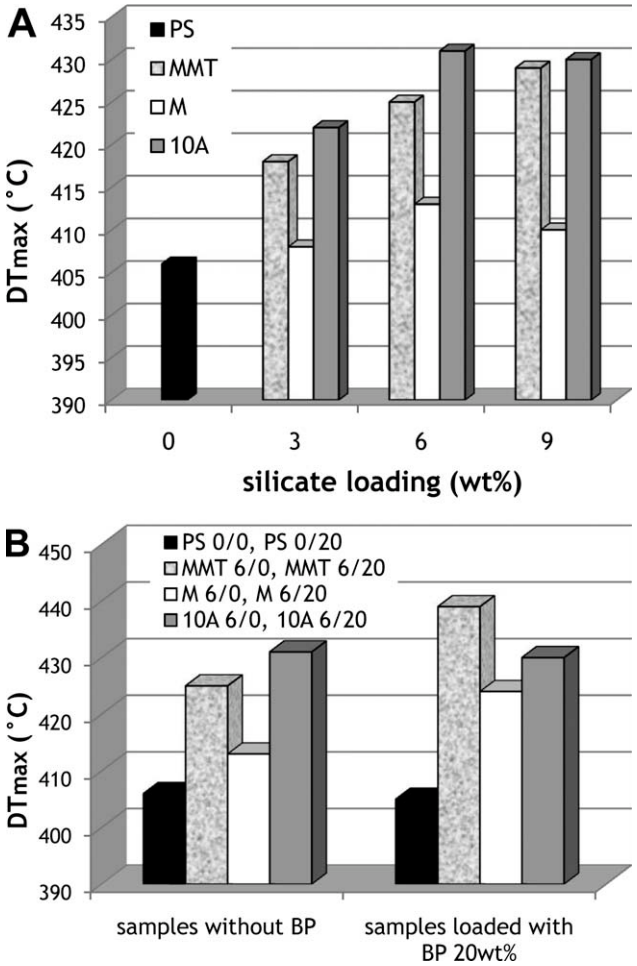

Figure 3 Effect of the system composition in terms of (A) silicate type and amount and (B) BP presence on DT_{max} of the PS–silicate nanocomposite microspheres.

CONCLUSIONS

The search of more and more flexible and tunable CR systems is a challenging issue that has attracted always increasing scientific and technological interest. In this respect, our work focused on the development and characterization of new organic–inorganic nanocomposite microparticles to verify their potential in the field of CR. The obtained results demonstrated that the sonication–solvent evaporation method is a ready, easy, and effective procedure for preparing nanostructured microparticulated CR carriers.

In this study, using this technique, we successfully produced PS–silicate nanocomposite microparticles containing different natural or organomodified lamellar silicates as nanofillers and BP as a model active agent. The adopted sonication–solvent evaporation method also assured high microparticle yields, adequate control of the size and shape of the prepared systems, and high incorporation efficiency (>84%) of the model active agent.

X-ray measurements evidenced that all formulations had intercalated polymer–silicate morphologies and that higher intercalation levels could be

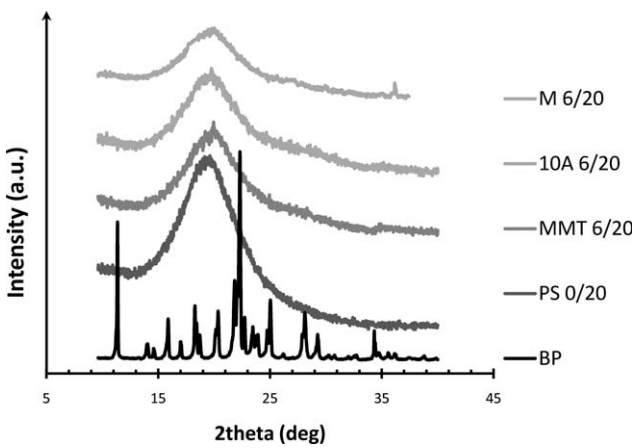

Figure 4 X-ray diffractograms of neat BP, BP-loaded PS microparticles, and all BP-loaded nanocomposite microparticles at 6 wt % silicate.

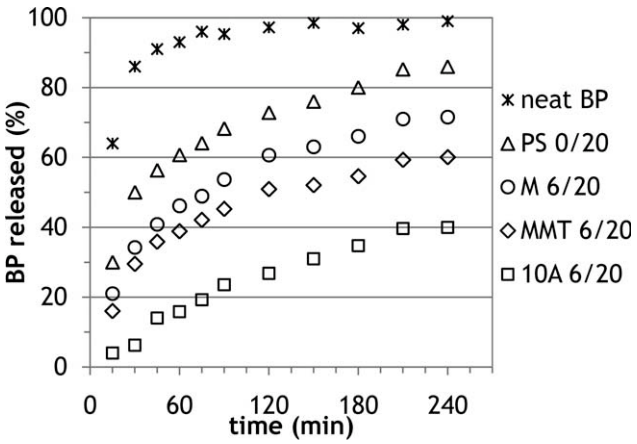

Figure 5 BP release profiles at 25°C from neat PS and PS–silicate nanocomposite microspheres with different compositions.

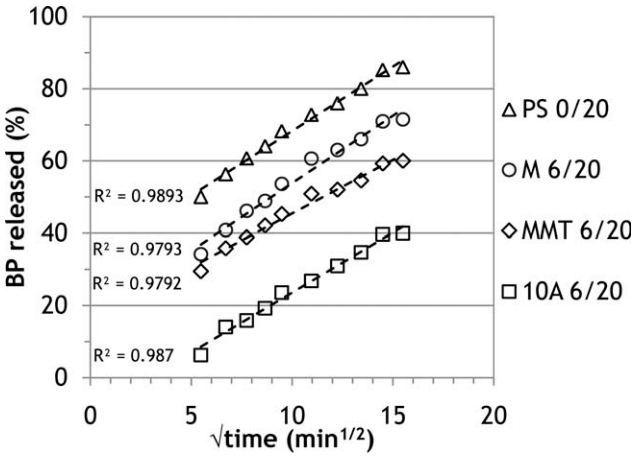

Figure 6 Kinetics of BP release (according to the Higuchi equation) at 25°C from the neat PS and PS–silicate nanocomposite microspheres with different compositions.

obtained with the 10A organomodified silicate, as could be expected on the basis of its higher affinity with the matrix compared to the other natural clays. As a result of the PS chain confinement in the silicate layers, the thermal resistances of all of the hybrids showed improvements in the range of 10–25°C. Moreover, because of the changes in the diffusion characteristics resulting from the silicate addition, the BP release profiles were significantly modified, being delayed compared to that of the unfilled PS microparticles. The release kinetics were markedly affected by the silicate nature; also, in this case, the 10A organoclay, which gave hybrids with a higher interlayer spacing and had higher affinities with both BP and PS, wielded the most effective slowing action.

References

1. Poncelet, D. In Surface Chemistry in Biomedical and Environmental Science, Eds.; Blitz, P.; Gunoko, V. M.; Springer: Berlin, 2006; p 23.
2. Microencapsulation: Methods and Industrial Applications; Benita, S., Ed.; Marcel Dekker: New York, 1996.
3. Ravi Kumar, M. N. V. Int J Pharm Pharm Sci 2000, 3, 234.
4. Scarfato, P.; Avallone, E.; Iannelli, P.; De Feo, V.; Acierno, D. J Appl Polym Sci 2007, 105, 3568.
5. Scarfato, P.; Avallone, E.; Iannelli, P.; Aquino, R. P.; Lauro, M. R.; Rossi, A.; Acierno, D. J Appl Polym Sci 2008, 109, 2994.
6. Arshady, R. Polym Eng Sci 2004, 30, 915.
7. Bao, W.; Zhou, J.; Luo, J.; Wu, D. J Microencapsul 2006, 23, 471.
8. Freitas, S.; Merkle, H. P.; Gander, B. J Controlled Release 2005, 102, 313.
9. Polymers for Controlled Drug Delivery; Tarcha, P. J., Ed.; CRC: Boca Raton, FL. 1991.
10. Choy, J.-H.; Jung, J.-S.; Oh, J.-M.; Park, M.; Jeong, J.; Kang, Y.-K.; Han, O.-J. Biomaterials 2004, 25, 3059.
11. bin Hussein, M. Z.; Yahaya, A. H.; Zainal, Z.; Kian, L. H. Sci Tech Adv Mater 2005, 6, 956.
12. Nakayama, H.; Kuwano, K.; Tsuhako, M. J Phys Chem Solids 2008, 69, 1552.
13. Shaikh, S.; Birdi, A.; Qutubuddin, S.; Lakatosh, E.; Baskaran, H. Ann Biomed Eng 2007, 35, 2130.
14. Kevadiya, B. D.; Joshi, G. V.; Bajaj, H. C. Int J Pharm Pharm Sci 2010, 388, 280.
15. Cypes, S. H. W.; Saltzman, M.; Giannelis, E. P. J Controlled Release 2003, 90, 163.
16. Wang, X.; Du, Y.; Luo, J. Nanotechnology 2008, 19, 065707.
17. Safety of Nanoparticles: From Manufacturing to Medical Applications; Webster, T. J., Ed.; Springer-Verlag: New York, 2008.
18. Kevadiya, B. D.; Joshi, G. V.; Patel, H. A.; Ingole, P. G.; Mody, H. M.; Bajaj, H. C. J Biomater Appl 2010, 25, 161.
19. Giannelis, E. P.; Krishnamoorti, R.; Manias, E. Adv Polym Sci 1999, 138, 107.
20. Toprak, M. S.; McKenna, B. J.; Waite, J. H.; Stucky, G. D. Chem Mater 2007, 19, 4263.
21. Duan, B.; Wang, M. Polym Degrad Stab 2010, 95, 1655.
22. Pitukmanorom, P.; Yong, T.-H.; Ying, J. Y. Adv Mater 2008, 20, 3504.
23. Takahashi, T.; Yamada, Y.; Kataoka, K.; Nagasaki, Y. J Controlled Release 2005, 107, 408.
24. Edgar, K. J. Cellulose 2007, 14, 49.
25. Higuchi, T. J Pharm Sci 1963, 52, 1145.